Resonance suppression and electromagnetic shielding effectiveness improvement of an apertured rectangular cavity by using wall losses*

Jiao Chong-Qing(焦重庆)† and Zhu Hong-Zhao(朱弘钊)

State Key Laboratory of Alternate Electrical Power System with Renewable Energy Sources, North China Electric Power University, Beijing 102206, *China*

(Received 16 December 2012; revised manuscript received 31 December 2012)

The cavity-mode resonance effect could result in significant degradation of the shielding effectiveness (SE) of a shielding enclosure around its resonance frequencies. In this paper, the influence of coated wall loss on the suppression of the resonance effect is investigated. For this purpose, an equivalent circuit model is employed to analyze the SE of an apertured rectangular cavity coated with an inside layer of resistive material. The model is developed by extending Robinson's equivalent circuit model through incorporating the effect of the wall loss into both the propagation constant and the characteristic impedance of the waveguide. Calculation results show that the wall loss could lead to great improvement on the SE for frequencies near the resonance but almost no effect on the SE for frequencies far away from the resonance.

Keywords: electromagnetic shielding, rectangular cavity, wall losses, resonance effect

PACS: 41.20.–q, 41.20.Jb, 84.32.–y **DOI:** 10.1088/1674-1056/22/8/084101

1. Introduction

Recently, there have been considerable concerns about the suppression of electromagnetic emission from electronic equipment and the improvement of equipment immunity.[1–8] One of the essential countermeasures for these purposes is electromagnetic shielding, which can be implemented by enclosing a piece of electronic equipment with a metallic enclosure. However, the shielding effectiveness (SE) of the enclosure can be reduced dramatically due to apertures that inevitably exist on the enclosure for some practical requirements like ventilation. Thus, lots of work has paid attention to the effect of apertures on shielding effectiveness, and some numerical,[3,4,9–11] analytic [6,12–14] or experimental results[6,7,11] have been reported.

Although the apertures are primarily responsible for the reduction of SE, the cavity-mode resonance can result in significant degradation of the SE at some resonance frequencies of the enclosure.[5,6,8] The rapid development of high-speed electronics and the wide applications of wireless communication technologies require that an enclosure is frequently used in an electromagnetic environment with frequencies up to 1 GHz. For many practical enclosures, these frequencies are higher than their fundamental resonant frequencies. As a result, the enclosure may behave like a cavity resonator and exhibits poor shielding performance at some resonant frequencies.

Earlier studies have shown that by using lossy materials to absorb the electromagnetic energy in the resonant cavity, the resonance phenomenon could be damped to some degree and the SE near resonant frequencies could be improved.[15–18] In Ref. [15], it was experimentally verified that the SE near resonance frequencies could be enhanced by placing a layer of lossy dielectric material in the back of an enclosure. Reference [16] shows that the resonance noise from a power bus structure can be suppressed by coating the power and ground planes with a thin layer of lossy magnetic material. In Ref. [17], an analytic formulation is presented to analyze the SE of an aperture-free spherical enclosure coated with resistive material, and the great enhancement of the SE is observed at many resonant frequencies, which are distributed discretely within a wide frequency bandwidth. In Ref. [18], it was experimentally demonstrated that by employing resistive material, the electromagnetic radiation from an apertured cavity with internal noise source can be reduced obviously not only for resonance frequencies but also for these frequencies away from the resonances.

In this paper, we present a simple circuit approach to evaluating the effect of conductive wall loss on the SE of an apertured rectangular enclosure under plane wave illumination. The approach is an extension of Robinson's equivalent circuit formulation.[6] In Robinson's formulation, the enclosure is modeled as a length of rectangular waveguide ended with a short circuit. The extension is carried out by incorporating the effect of wall loss into both the propagation constant and the characteristic impedance of the waveguide. The boundary impedance perturbation method is used to deduce the propagation constant of the electromagnetic mode in a rectangular waveguide with an imperfect conducting wall. Since the perturbation method is not applicable for the case of dielectric

*Project supported by the National Natural Science Foundation of China (Grant No. 51037001).

†Corresponding author. E-mail: cqjiao@ncepu.edu.cn

© 2013 Chinese Physical Society and IOP Publishing Ltd

or magnetic wall loss, the circuit approach presented here is only applicable to conductive wall loss. In order to validate the effectiveness of the presented approach, numerical results from the finite element method based software HFSS[19] are also reported for comparison. The rest of the present paper is organized as follows. The circuit approach is described in Section 2, the propagation constant is deduced in Section 3, the results and discussion are presented in Section 4, and some conclusions are drawn from the present study in Section 5.

2. Equivalent circuit model

Figure 1 shows a metallic rectangular cavity with a rectangular aperture illuminated by a normally incident plane wave with its E field parallel to the x axis. The length, height, width, and wall thickness of the cavity are a, b, d, and t, respectively. The length and width of the aperture are l and w, respectively. The SE observation point P is located at $(b/2, a/2, p)$ with p denoting the distance form point P to the aperture. The dimensions of the cavity are $a = 300$ mm, $b = 120$ mm, $d = 300$ mm, and $t = 0.5$ mm. The dimensions of the aperture are $l = 100$ mm and $w = 5$ mm.

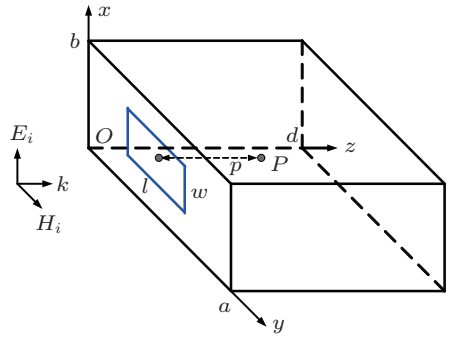


Fig. 1. (color online) Apertured rectangular cavity under plane wave illumination.

The equivalent circuit model presented by Robinson to analyze the field coupling into the cavity through the aperture is shown in Fig. 2.[6] In this model, the incident wave is represented by a voltage source v_0 and the vacuum wave impedance Z_0. The aperture is represented by a length of coplanar transmission line shorted at each end with phase constant $k_0 = 2\pi/\lambda$ and characteristic impedance Z_{0s} like[6,20]

$$Z_{0s} = 120\pi^2 \left[\ln\left(2\frac{1+\sqrt[4]{1-(w_e/b)^2}}{1-\sqrt[4]{1-(w_e/b)^2}} \right) \right]^{-1}, \quad (1)$$

where λ is the free space wavelength and $w_e = w - 5t[1 + \ln(4\pi w/t)]/4\pi$ is the effective width of the slot. The cavity is considered as a waveguide shorted at the end $z = d$ and is modeled by an equivalent transmission line of the TE_{10} waveguide mode with characteristic impedance Z_g and axial wavenumber k_g expressed as

$$k_g = k_0\sqrt{1-(\lambda/2a)^2}, \quad (2)$$

$$Z_g = Z_0 \times k_0/k_g. \quad (3)$$

When the wave frequency is below the cutoff frequency of the second lowest waveguide mode (TE_{20}), this model gives the results in good agreement with experimental measurements and numerical simulations.[6]

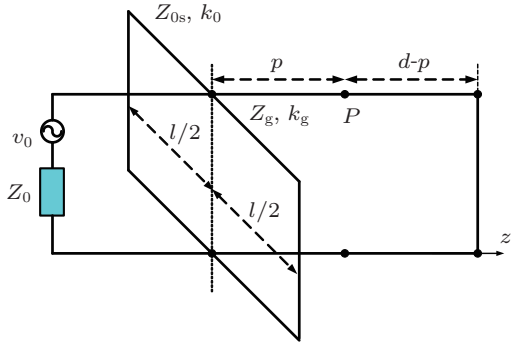


Fig. 2. (color online) Equivalent circuit of the apertured rectangular cavity under plane wave illumination.

The voltage and current at P are denoted by v_p and i_p, respectively. If the cavity is removed, the corresponding voltage and current at P are represented by v'_p and i'_p, respectively, where $v'_p = v_0/2$ and $i'_p = v_0/2Z_0$. Then, the electric and magnetic shielding effectiveness at the observation point P are defined as, respectively

$$S_E = -20\log_{10}|v_p/v'_p| = -20\log_{10}|2v_p/v_0|, \quad (4)$$

$$S_H = -20\log_{10}|i_p/i'_p| = -20\log_{10}|2i_pZ_0/v_0|. \quad (5)$$

In this paper, the above equivalent circuit model is extended to account for the effect of loaded wall loss. Now, we assume that the four sidewalls of the cavity ($x = 0$, $x = b$, $y = 0$, and $y = a$) are no longer lossless, but loaded with resistive material, which will change the values of Z_g and k_g, and hence influence the shielding effectiveness. In the following, the expression of the propagation constant in a lossy rectangular waveguide will be deduced. Then, the corresponding characteristic impedance can also be obtained by using Eq. (3), which describes the relationship between propagation constant and characteristic impedance. Once the propagation constant and characteristic impedance are replaced with the corresponding values in the case of the lossy waveguide, the S_E and S_H corresponding to the lossy case can be calculated by using the extended circuit model.

3. Propagation constant of a lossy rectangular waveguide

When the inner wall of a waveguide is coated with conductive material with low conductivity, the magnitude of electromagnetic waves will decrease along the waveguide axis following an exponential function. Usually, the attenuation constant is calculated by the power loss method.[21] For the rectangular waveguide shown in Fig. 1, the power loss method gives the attenuation constant α for any TE$_{mn}$ mode like[21,22]

$$\alpha = \frac{c\delta k_0^2}{4\pi\sqrt{f^2-f_c^2}}\left[\frac{k_{c0}^2}{k_0^2}\cdot\frac{\delta_n a+\delta_m b}{ab} + \left(1-\frac{k_{c0}^2}{k_0^2}\right)\frac{\delta_m n^2 a+\delta_n m^2 b}{n^2a^2+m^2b^2}\right], \quad (6)$$

where f is the wave frequency, f_c is the cutoff frequency, $k_{c0}=\sqrt{k_x^2+k_y^2}$ is the cutoff wavenumber of the TE$_{mn}$ mode with $k_x=m\pi/a$ and $k_y=n\pi/b$, $\delta=\sqrt{2/(\omega\sigma\mu_0)}$ is the skin depth in the lossy material, $\omega=2\pi f$, σ and μ_0 denote the conductivity and permeability of the lossy material respectively, and

$$\delta_m=\begin{cases}2, & m\neq 0,\\ 1, & m=0,\end{cases}\qquad \delta_n=\begin{cases}2, & n\neq 0,\\ 1, & n=0.\end{cases} \quad (7)$$

Equation (6) shows that when $f<f_c$, α is an imaginary number and when $f=f_c$, α tends to be infinite. Therefore, equation (6) is only feasible on condition that the wave frequency is larger than the cutoff frequency. In addition, the power loss method cannot consider the effect of wall loss on phase constant. In practice, the frequency of electromagnetic interference may be lower than the cutoff frequency. So, a formula of propagation constant feasible for frequencies below cutoff is desired. Based on the boundary impedance perturbation method, and assuming a propagation form of $e^{j\omega t-\gamma z}$, a general formula for propagation constant γ of any TE$_{mn}$ mode is presented as[23,24]

$$\gamma^2=-\beta_0^2-(1-j)\frac{\delta}{2}\frac{\oint_C\left(k_{c0}^4|\phi_0|^2+\beta_0^2\left|\frac{\partial\phi_0}{\partial\hat{l}}\right|^2\right)dl}{k_{c0}^2\iint_S|\phi_0|^2\,ds}, \quad (8)$$

where $\beta_0=\sqrt{k_0^2-k_{c0}^2}$, S is the cross section of the waveguide, C is the boundary curve of S, and ϕ_0 represents the distribution of the axial magnetic component of the TE$_{mn}$ mode over the cross section. It should be noted that equation (8) is not only applicable for rectangular waveguides, but also for the waveguides with uniform cross section like cylindrical or coaxial waveguides. For a rectangular waveguide,

$$\phi_0=\cos(k_x x)\cos(k_y y), \quad (9)$$

and hence,

$$\gamma^2=-\beta_0^2-(1-j)\delta\left\{\frac{\delta_m}{a}\left(k_{c0}^2+\beta_0^2\frac{k_y^2}{k_{c0}^2}\right)+\frac{\delta_n}{b}\left(k_{c0}^2+\beta_0^2\frac{k_x^2}{k_{c0}^2}\right)\right\}. \quad (10)$$

Assuming that $\gamma=\alpha+j\beta$, α is the attenuation constant and β is the phase constant. When $f>f_c$, let $\gamma=j\beta_0+\Delta\gamma$ and $|\beta_0|\gg|\Delta\gamma|$, then we could deduce an approximate solution of $\Delta\gamma$, and further an approximate attenuation constant like

$$\alpha\approx\delta(2\beta_0)^{-1}\left\{\frac{\delta_m}{a}\left(k_{c0}^2+\beta_0^2\frac{k_y^2}{k_{c0}^2}\right)+\frac{\delta_n}{b}\left(k_{c0}^2+\beta_0^2\frac{k_x^2}{k_{c0}^2}\right)\right\}. \quad (11)$$

It is easy to prove that equation (11) is identical to Eq. (6). So, for frequencies above cutoff, the two methods produce the same result.

For $\sigma=10^4$ S/m, figure 3 shows the effect of the wave frequency on the attenuation constant obtained from the two different methods. It can be seen that once f is a little larger than the cutoff frequency f_c, the results from the two methods are in good agreement with each other. Thus, in the following, equation (10) is adopted since it is also applicable for frequencies below cutoff.

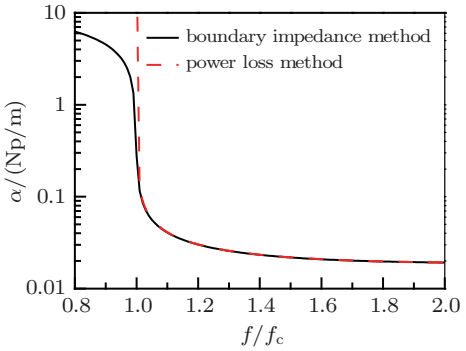


Fig. 3. (color online) Comparison between the attenuation constants obtained from the power loss method with those obtained from the boundary impedance perturbation method.

4. Results and discussion

4.1. Attenuation constant and phase constant

Figures 4 and 5 show, respectively, the attenuation and phase constants of the TE$_{10}$ wave versus frequency for four different conductivities. It can be found that with the decrease of conductivity, the attenuation constant increases for frequencies near and above the cutoff and decreases slightly for frequencies below the cutoff. However, the phase constant always increases in the whole frequency range with conductivity decreasing. With the loss loaded, the phase constant is non-zero for frequencies below cutoff, which means that the wave is not purely evanescent but propagating. The validation of the boundary impedance perturbation method requires $\sigma/\varepsilon\omega\gg 1$. Obviously, this condition can be satisfied even for the minimal conductivity of 10 S/m and the highest frequency of 1 GHz.

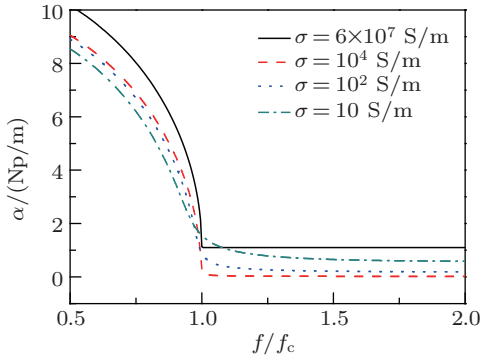


Fig. 4. (color online) Plots of attenuation constant versus frequency for four different conductivities.

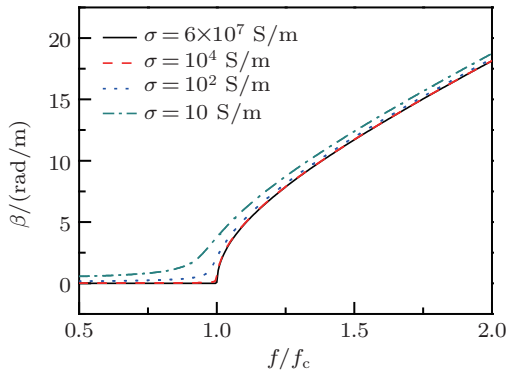


Fig. 5. (color online) Plots of phase constant versus frequency for four different conductivities.

4.2. Validation of the results

By using γ given in Eq. (10) to replace k_g in Eqs. (2) and (3) in the form of $k_g = -j\gamma$, the circuit model for lossless cavity is extended to the case of lossy cavity. Then, the S_E in the case of lossy cavity can be calculated. First, we take the lossless case for comparison. For $f = 707$ MHz, figure 6 gives a comparison between the S_E distribution along the central line ($x = 60$ mm, $y = 150$ mm, $0 < p < 300$ mm) obtained from the circuit model and that from the HFSS software. As shown in the figure, the S_E depends strongly on the value of p, that is, the position of the observation point. The S_E is smaller in the central region and larger near front and back walls. The underlying reason consists in the standing-wave field distribution of the TE_{101} cavity mode. When $p > 25$ mm, the simulation and calculation are nearly identical. When $p < 25$ mm, the circuit method is no longer applicable and there is obvious difference between the two curves, because the circuit model neglects the effects of high-order evanescent modes which exist mainly near the aperture.

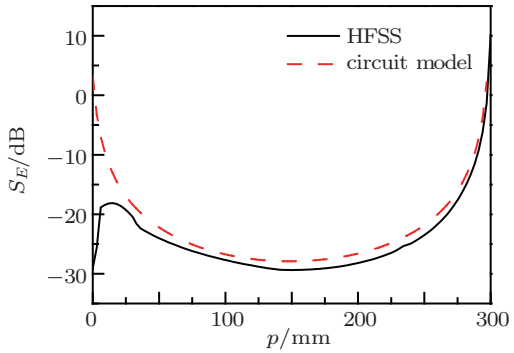


Fig. 6. (color online) Simulated and calculated S_E versus the position of observation point for $f = 707$ MHz.

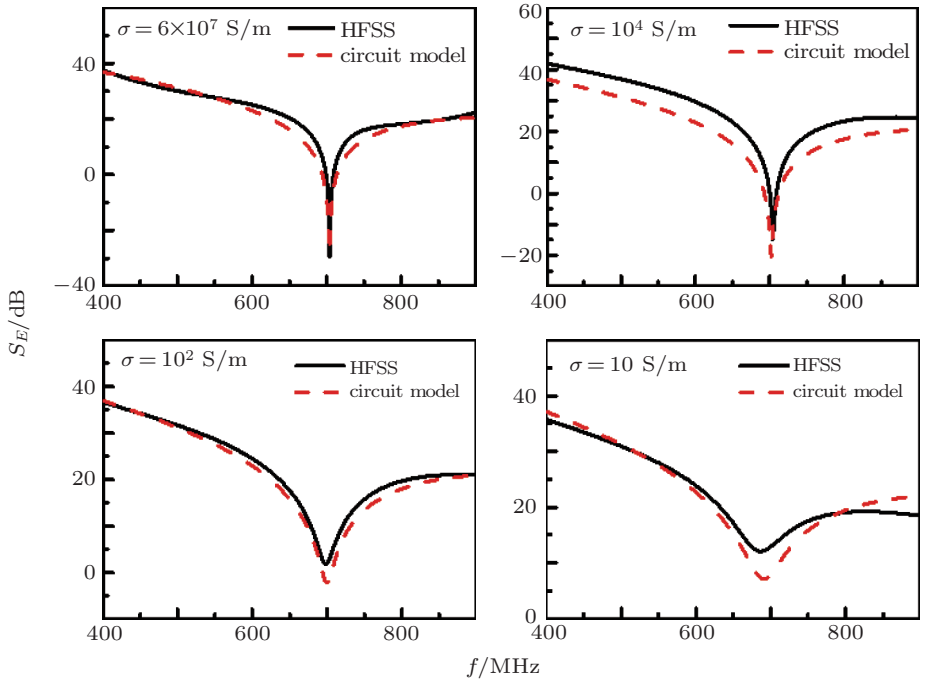


Fig. 7. (color online) Plots of simulated S_E and calculated S_E versus frequency with $p = 150$ mm for different conductivities.

Second, we consider the lossly case. Figure 7 shows the simulated and calculated S_E at the observation point (60 mm, 150 mm, 150 mm) for four different conductivities of 6×10^7 S/m, 10^4 S/m, 10^2 S/m, and 10 S/m. The two curves are in good consistence in the frequency range from 400 MHz to 900 MHz. By and large, the maximum error between the circuit model and HFSS is about 5 dB. The S_E reduction sharply at about 700 MHz is observed clearly, which is due to the resonance effect of the TE_{101} cavity mode. The TE_{101} cavity mode is the first axial resonance mode of the TE_{10} waveguide mode, and all other TE_{10n} cavity modes can be considered as the high order axial resonance modes of the TE_{10} waveguide mode.

It can be seen that with conductivity declining in the order: 6×10^7 S/m, 10^4 S/m, 10^2 S/m, and 10 S/m, the minimal S_E which happens at the resonance frequency increases -28 dB, -20 dB, -2 dB, and 7 dB correspondingly. In addition, the resonance frequency corresponding to the minimal S_E will also reduce gradually. When $\sigma = 10$ S/m, a strong resonance suppression effect can be achieved. However, we cannot conclude that the S_E can be improved unlimitedly by lowering the conductivity infinitely. In fact, there must be an optimum conductivity since conductivities of zero and infinity both mean no lossless. However, this optimum conductivity may not be found by the present model since the optimum conductivity is usually so low that the premise ($\sigma \gg \omega\varepsilon$) of using boundary impedance perturbation method is no longer valid.

4.3. Magnetic shielding effectiveness

Figure 8 illustrates the dependences of the magnetic shielding effectiveness S_H on wave frequency at $p = 150$ mm for the four different conductivities. It can be seen that with the decrease of the conductivity, the minimal S_H corresponding to the resonance frequency is enhanced obviously while the maximal S_H corresponding to the node of the magnetic field is lowered. As a result, the curve corresponding to $\sigma = 10$ S/m is approximately flat around the resonance frequency.

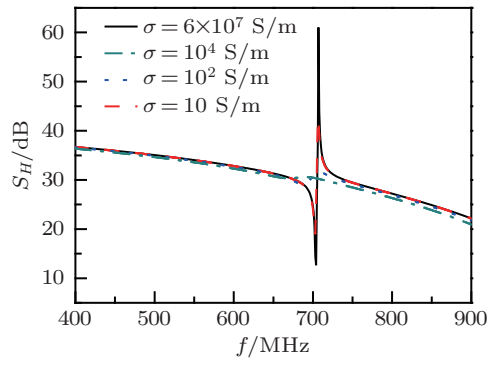


Fig. 8. (color online) Plots of magnetic shielding effectiveness versus frequency at $p = 150$ mm for four different conductivities.

4.4. Suppression effect at higher frequencies

In Fig. 9, the frequencies are extended to 2 GHz. As shown in the figure, the resonant suppression at higher frequencies is also effective. Of course, if only TE_{10} mode is considered, the above model may not be feasible for frequencies above 1 GHz since a high order mode like TE_{20} may occur. However, this figure can convey to us the information that the wall loss is also effective for suppressing high-order cavity resonance modes like TE_{102} near 1.1 GHz, TE_{103} near 1.6 GHz, and slot resonance mode near 1.5 GHz. Hence, we can guess that the lossy layer may also be feasible for damping other types of high-order resonance modes.

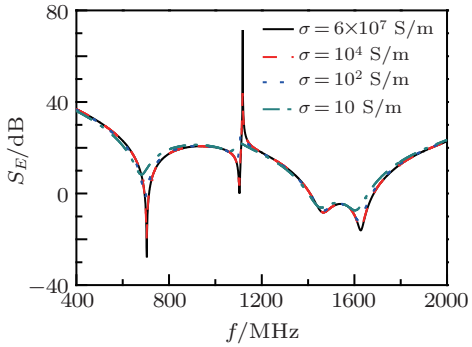


Fig. 9. (color online) Variations of electric shielding effectiveness at $p = 150$ mm with frequency in a range from 0.4 GHz to 2 GHz for the four different conductivities.

4.5. Effect of the back wall loss

When the back wall ($0 < x < 120$ mm, $0 < y < 300$ mm, $z = 300$ mm) is also coated, the right end of the equivalent transmission line shown in Fig. 2 is no longer shorted but is terminated with a load impedance Z_L like[21,23]

$$Z_L = (1+\mathrm{j})\sqrt{\frac{\omega\mu}{2\sigma}}, \tag{12}$$

which is essentially the surface impedance of a layer of conductive material. Let S'_E denote the electric shielding effectiveness when the back wall is coated, figure 10 gives a comparison between S'_E and S_E. It can be seen that S'_E is a little

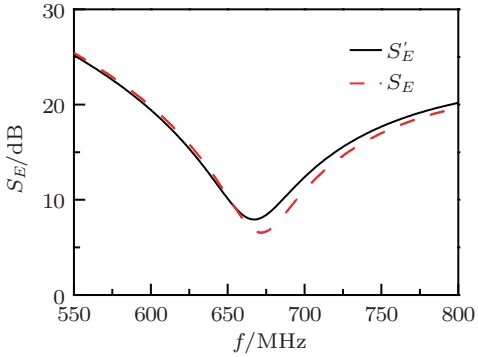


Fig. 10. (color online) Comparison between S'_E and S_E at $p = 150$ mm with σ=10 S/m.

larger than S_E near the resonant frequency. So, the shielding effectiveness can be improved a little if the back wall is also coated with lossy material. Of course, it may also be enhanced further if the front wall is also lossy. However, this case cannot be considered in the present model.

4.6. Thickness of the lossy material

Up to now, we have not considered the effect of the lossy layer thickness t_0. In other words, we have assumed that the thickness is larger than the skin depth. However, when the thickness is smaller than the skin thickness, its effect must be considered. According to Ref. [25], the effect of lossy layer thickness can be taken into account by adding a so-called thickness factor $\mathrm{j}\times\tan[(1-\mathrm{j})t_0/\delta]$ into the propagation constant in Eq. (10) as

$$\gamma^2 = -\beta_0^2-(1-\mathrm{j})\delta\left\{\frac{\delta_m}{a}\left(k_{c0}^2+\beta_0^2\frac{k_y^2}{k_{c0}^2}\right)+\frac{\delta_n}{b}\left(k_{c0}^2+\beta_0^2\frac{k_x^2}{k_{c0}^2}\right)\right\}\times\mathrm{j}\times\tan((1-\mathrm{j})t_0/\delta). \quad (13)$$

Based on this equation, figure 11 displays the dependences of the S_E on frequency for four different thickness values with $\sigma = 10$ S/m. It is shown that the S_E will increase with thickness increasing when the thickness is smaller than the skin depth. However, once the thickness is larger than the skin depth, the S_E will tend to be steady.

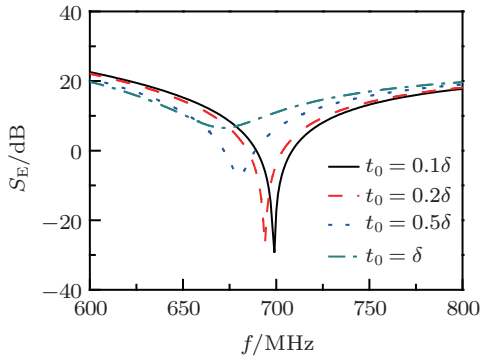


Fig. 11. (color online) Calculated values of S_E at $p = 150$ mm for four different thickness values with σ=10 S/m.

5. Conclusions

According to the boundary impedance perturbation method, in this paper an analytical formula for the propagation constant of electromagnetic mode in a lossy rectangular waveguide is derived. The formula is applicable not only for frequencies above cutoff but also for frequencies near and below cutoff. This propagation constant then is inserted into the Robinson's equivalent circuit model to investigate the effect of resistive wall loss on the suppression of shielding effectiveness reduction resulting from the cavity resonance effect. The results from the presented circuit model are in good agreement with those from the full-wave software HFSS. The results show that wall loss can clearly improve the shielding effectiveness around the resonant frequencies but has negligible effect for other frequencies. The results are helpful for guiding the design of electromagnetic shielding cavities. However, dielectric and magnetic losses cannot both be treated in the present model, which will be considered in future research.

References

[1] Wu J and Xiao C Y 2010 *Chin. Phys. B* **19** 044101
[2] Zhang S Q and Wu Q 2013 *Acta Phys. Sin.* **62** 029202 (in Chinese)
[3] Audone B and Balma M 1989 *IEEE Trans. Electromagn. Compat.* **31** 102
[4] Wang T, Harrington R F and Mautz J R 1990 *IEEE Trans. Antennas Propag.* **38** 1805
[5] Zhang S Q 2012 *Chin. Phys. B* **21** 065101
[6] Robinson M P, Benson T M, Christopoulos C, Dawson J F, Ganley M D, Marvin A C, Porter S J and Thomas D W P 1998 *IEEE Trans. Electromagn. Compat.* **40** 240
[7] Shim J J, Kam D G, Kwon J H and Kim J 2010 *IEEE Trans. Electromagn. Compat.* **52** 566
[8] Jiao C Q 2012 *IEEE Trans. Electromagn. Compat.* **54** 696
[9] Wang J G, Qu H M, Fan R Y, Chen Y S and Zhang T B 1994 *High Power Laser and Particle Beams* **6** 282
[10] Chen J and Wang J G 2007 *IEEE Trans. Electromagn. Compat.* **49** 354
[11] Wang J G, Liu G Z and Zhou J S 2003 *High Power Laser and Particle Beams* **15** 1093
[12] Dehkhoda P, Tavakoli A and Moini R 2008 *IEEE Trans. Electromagn. Compat.* **50** 208
[13] Jiao C Q and Qi L 2012 *Acta Phys. Sin.* **61** 134104 (in Chinese)
[14] Azaro R, Caorsi S, Donelli M and Gragnani G L 2002 *IEEE Trans. Microw. Theory Tech.* **50** 2259
[15] Olyslager F, Laermans E, Zutter D D, Criel S, Smedt R D, Lietaert N and Clercq A D 1999 *IEEE Trans. Electromagn. Compat.* **41** 202
[16] Wu L K and Tseng C H 2005 *IEEE Trans. Electromagn. Compat.* **47** 731
[17] Yamane T, Nishikata A and Shimizu Y 2000 *IEEE Trans. Electromagn. Compat.* **42** 441
[18] Li M, Drewniak J L, Hubbing T H, Dubroff R D and Vandoren T P 2000 *IEEE Trans. Electromagn. Compat.* **42** 135
[19] Ansoft HFSS 10.0 [online] Available: http//www.ansoft.com/products/hf/hfss/
[20] Gupta K C, Garg R and Bahi I J 1979 *Microstrip Lines and Slotlines* (Norwood, MA: Artech House)
[21] Zhang K Q and Li D J 2001 *Electromagnetic Theory for Microwave and Optoelectronics*, 2nd edn. (Beijing: Electronic Industry Press) (in Chinese)
[22] Robert E Collin 1991 *Field Theory of Guided Waves*, 2nd edn. (New York: Wiley Interscience)
[23] Jackson J D 1975 *Classical Electrodynamics*, 2nd edn. (New York: Wiley Interscience)
[24] Jiao C Q 2011 *Prog. Electromag. Res. Lett.* **22** 119
[25] Luo J R and Jiao C Q 2006 *Appl. Phys. Lett.* **88** 061115